The Effect of Two Receivers on Broadcast Molecular Communication Systems

Yi Lu , Matthew D. Higgins, *Senior Member, IEEE,* Adam Noel, *Member, IEEE,* Mark S. Leeson, *Senior Member, IEEE* and Yunfei Chen, *Senior Member, IEEE*

***Abstract* – Molecular communication is a paradigm that utilizes molecules to exchange information between nano-machines. When considering such systems where multiple receivers are present, prior work has assumed for simplicity that they do not interfere with each other. This paper aims to address this issue and shows to what extent an interfering receiver, R_I, will have an impact on the target receiver, R_T, with respect to Bit Error Rate (BER) and capacity. Furthermore, approximations of the Binomial distribution are applied to reduce the complexity of calculations. Results show the sensitivity in communication performance due to the relative location of the interfering receiver. Critically, placing R_I between the transmitter T_X and R_T causes a significant increase in BER or decrease in capacity.**

***Index Terms*— Bit Error Rate, Broadcast Channel, Channel Capacity, Diffusion-based Molecular Communications.**

I. INTRODUCTION

MOLECULAR communication is a recently established paradigm that utilizes molecules to exchange information between nano-machines [1]. In a fluidic medium, with no drift, the essential premise is that the information molecules are released at the transmitter and then propagate via diffusion until they reach a receiver where it will be absorbed and removed from the environment. To date, there have been several key papers that address the characteristics of the channel for point to point (PTP) transmission systems, for example [2]–[7]. However, scenarios where multiple transmitters communicate with multiple receivers, such as the multi-access channel or the broadcast channel in molecular communication, have not yet received as much attention as the topic deserves. Existing papers on this subject include [8]–[12]. Given the scale of work regarding the broadcast channel in conventional communication systems, and the prevalence of multiple-input multiple-output in natural molecular communication system [9], [10], this knowledge gap within molecular communication systems is thus important to redress.

The investigations in [11] and [12] aimed to analyze the broadcast channel where a single transmitter communicates with multiple receivers and provided subsequent capacity calculations. However, the current literature generally assumes that the signal at each receiver is independent, receiving molecules as if other receivers were not present, i.e. effectively treating the system as multiple PTP communication channels. Unlike conventional Radio Frequency (RF) electromagnetic communications where the receivers are generally regarded as not being able to interfere with each other [13], for a molecular communication system with multiple absorbing receivers, the receivers do interfere with each other as the absorbed molecule cannot be captured by any other receivers.

In this paper, in order to investigate how the receivers influence each other, we consider a communication system with one transmitter and two receivers. As shown in Fig. 1, one transmitter, T_X emits molecules into a channel with two identical receivers that can absorb the same type of molecule. One receiver is defined as the target receiver, R_T, whilst the other is defined as the interfering receiver, R_I. If we use the independence assumptions of [11] and [12], then there would be no molecule 'sink' or 'absorption' component caused by the presence of the interferer. This further implies that the performance of the system with respect to the target receiver is

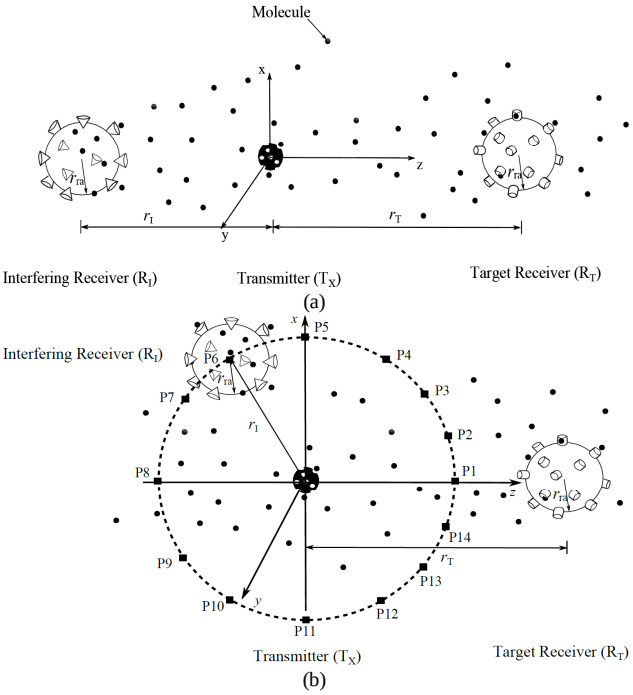

Fig. 1. Molecular communication system with two absorbing receivers. (a) R_I is placed on the *z*-axis. (b) R_I is placed on a circle.

Yi Lu, Mark S. Leeson and Yunfei Chen are with the School of Engineering, University of Warwick, Coventry, CV4 7AL, UK.

Matthew D. Higgins is with the WMG, University of Warwick, Coventry, CV4 7AL, UK.

Email: {yi.lu; m.higgins; mark.leeson; yunfei.chen}@warwick.ac.uk.

Adam Noel is with the School of Electrical Engineering and Computer Science, University of Ottawa, Ottawa, ON, K1N 6N5, Canada.

Email: anoel2@uottawa.ca.

Manuscript accepted: 13 October 2016.

likely to be overestimated.

This paper aims to clearly show the influence of R_I on R_T as a function of their relative positions. In this paper, two studies of the effects of positions of R_I on R_T are presented, see Figs. 1(a) and (b). For both studies, a fixed position of T_X and R_T is considered. Fig. 1(a) shows the first study, where R_I and R_T are centered on the same line, i.e. fixed *x* and *y* coordinates. Each receiver's location is defined by the *z*-coordinate of its center. Three positions of R_I will be investigated. Scenario 1 considers that R_I is located to the left of both T_X and R_T. Scenario 2 considers that R_I is between T_X and R_T. Finally, Scenario 3 considers that R_I is located to the right of both T_X and R_T. Fig. 1(b) shows another study, where the positions of T_X and R_T are the same as the first study, however, R_I is placed on a circle that is centered at the origin and the radius of this circle is the distance between T_X and R_I. In this study, four scenarios are investigated, the details of which are given in Section V. At each of these positions the impact on the Bit Error Rate (BER) and channel capacity of the communication link between T_X and R_T, which can be represented as the target link, will be shown.

This paper will therefore present and contribute the following:

- Firstly, a two-receiver broadcast communication channel with a three-dimensional diffusion-based propagation model is simulated for a molecular communication system with absorbing receivers. One of the important parameters of performance analysis, capture probability, can be obtained through this simulation. According to the analysis of capture probability, interference exists between the two receivers, and each communication channel should therefore not be simply modeled as a PTP channel. It is believed that this is the first paper to show this in the literature.
- Secondly, the channel model is analytically studied for molecular communications, where a detailed explanation and derivation of the arrival model is provided to help the reader more easily understand why and how to use this model. Furthermore, the expressions for BER and channel capacity are derived with the consideration of an arbitrary length of Inter Symbol Interference (ISI).
- Thirdly, two studies of the positions of R_I are presented. First, the position of R_I is studied by varying its location on the *z*-axis. Second, the position of R_I is changed along a circle. Thus, the study of positions of R_I includes both one-dimensional case and two-dimensional case.
- Finally, the impact of the introduction of the interfering receiver with respect to its relative location is investigated by analyzing the performance of the target link.

The remainder of this paper is organized as follows. The diffusion-based molecular communication model is given in Section II. The channel model is investigated in Section III. In Section IV and Section V, the numerical results for both studies are presented and analyzed. Finally, the paper is concluded in Section VI.

II. Diffusion –Based Molecular Communication Model

In this work, the three-dimensional random walk is used to describe the molecular diffusion process. If the Cartesian coordinates of the k^{th} molecule at time t are $(x_k(t), y_k(t), z_k(t))$, then the coordinates of this molecule at time $t+\Delta t$ are given by [14]:

$$x_k(t+\Delta t) = x_k(t) + \zeta_1\sqrt{2D\Delta t}, \quad (1)$$

$$y_k(t+\Delta t) = y_k(t) + \zeta_2\sqrt{2D\Delta t}, \quad (2)$$

$$z_k(t+\Delta t) = z_k(t) + \zeta_3\sqrt{2D\Delta t}, \quad (3)$$

where ζ_1, ζ_2 and ζ_3 are independent random numbers sampled from a Gaussian distribution with mean 0 and variance 1. D is the diffusion coefficient and Δt is the time step.

A number of molecules are released as an impulse at the beginning of each time slot from coordinates (x_0, y_0, z_0) (i.e., (0, 0, 0)). For the diffusion process, each molecule executes a random walk in three-dimensional space that follows (1)-(3), and each one moves independently of all other molecules [14]. For the reception process, a molecule is absorbed if it is within one of the receivers at the end of a time step. Once it has been absorbed, it is eliminated. The receiver can decode the information by counting the number of received molecules at the end of the time slot. In this work, we assume that the transmitter and receiver are synchronized [15], [16] and receivers can count the number of received molecules during a time slot [10].

The ability that a molecule can be captured by the receiver is denoted as the capture probability. The expression of the capture probability for a PTP molecule communication system is given in [17]. However, the analytical expressions for the capture probability with respect to time for the multi-receiver system are still unknown. Therefore, here, the capture probability for each receiver is obtained via simulation process.

In the simulation, the number of received molecules at each receiver in 10^5 trials can be obtained by taking a large time slot duration, t_s, (5000s). Thus, the capture probability of a molecule at a receiver can be calculated using the number of received molecules divided by the total number of trials.

The simulation process has been compared with the model for two absorbing spheres in [18] to validate the correct behavior of the simulation process. There, the authors introduced a scenario where molecules located at coordinates (0, 0, *z*) diffuse to a pair of receivers S_1 and S_2 located at (0, 0, *l*/2) and (0, 0, -*l*/2) respectively, where *l* is an arbitrary distance. For this scenario, the analytical and approximation capture probabilities for S_1 and S_2 are given when the diffusion time is large enough (i.e., as $t \to \infty$). Comparisons in [18] show a strong agreement between the analytical and the approximation results. Thus, only the asymptotic capture probabilities found using the approximate expressions are compared with simulation in this work.

The approximations for capture probability $p_{1,\text{ap}}$ with S_1 and $p_{2,\text{ap}}$ with S_2 were introduced as [18, Eq. (4.20)]:

$$p_{1,\text{ap}} = r_{\text{ra}} \Big/ \left(r_1 \times \left(1 - \left(r_{\text{ra}}/l\right)^2\right)\right) - r_{\text{ra}}{}^2 \Big/ \left(r_2 \times l \times \left(1 - \left(r_{\text{ra}}/l\right)^2\right)\right), \quad (4)$$

$$p_{2,\mathrm{ap}} = r_{\mathrm{ra}} \Big/ \left(r_2 \times \left(1-\left(r_{\mathrm{ra}}/l\right)^2\right)\right) - {r_{\mathrm{ra}}}^2 \Big/ \left(r_1 \times l \times \left(1-\left(r_{\mathrm{ra}}/l\right)^2\right)\right). \quad (5)$$

where r_{ra} is the radius of the receivers, r_1 and r_2 are the distances between the T_X and the centers of the two receivers.

As shown in Fig. 2, the capture probabilities found using the approximate expressions (4) and (5) are compared with the simulation results. The parameters used in this comparison agree with [3] and [18], where $l = 4\mu\mathrm{m}$, $r_{\mathrm{ra}} = 0.31487\mu\mathrm{m}$, and $D = 79.4\mu\mathrm{m}^2\mathrm{s}^{-1}$.

The R-square coefficient [19] of determination is introduced to measure the goodness of fit between simulation results and results from approximations. The closer this value is to 1, the better the fit of the simulation is, and is given by:

$$\mathrm{R}^2 = 1 - \mathrm{SSE}/\mathrm{SST}, \quad (6)$$

where SSE is the sum of squared errors of prediction and SST is the sum of squares of the difference between the dependent variable and its mean. The R-square for S_1 and S_2 are 0.9935 and 0.9910 respectively. This comparison confirms that the results from this simulation process are accurate.

III. Channel Analysis

The influence of R_I on R_T can be reflected in the performance of the target link. Thus, the focus here is the analysis of the target link.

The value of t_s used in Section II is too large to be used in a communication system. Thus, this value can be determined by finding the time at which 60% of molecules arrives at the R_T [3]. The capture probability for R_T within one time slot, $P_T(r_T, t_s)$, can be recomputed via the same simulation process introduced in Section II, where r_T is the distance between the T_X and R_T.

Considering an on-off keying modulation scheme, the system transmits information via the release, or not, of molecules from the T_X. A '1' is represented by a specific number of molecules released from the T_X, and '0' is represented by an absence of released molecules. At the receiver, when the number of molecules exceeds a pre-designed threshold τ, the symbol is denoted as a '1'; otherwise, denoted as a '0'. Considering that N information molecules are released as an impulse at the start of the time slot, the threshold τ can be determined by finding the minimum BER for $\tau \in [1, N]$.

Following [3], the number of molecules received by the receiver out of the current N molecules released in the current time slot, N_0, follows a Binomial distribution:

$$N_0 \sim \boldsymbol{B}\left(N, P_{\mathrm{T}}\left(r_{\mathrm{T}}, t_{\mathrm{s}}\right)\right). \quad (7)$$

The transmitted molecules cannot be guaranteed to reach the receiver within one time slot, which can cause ISI. In this work, we consider a memory channel with an ISI length I. Molecules that do not reach a receiver within one time slot may arrive in a future time slot. We denote N_i as the number of molecules that were released at the start of the i^{th} time slot before the current one and arrive in the current time slot.

Consider that N_i ($N_i = y$) interfering molecules are received in the current time slot amongst those remaining molecules. Thus

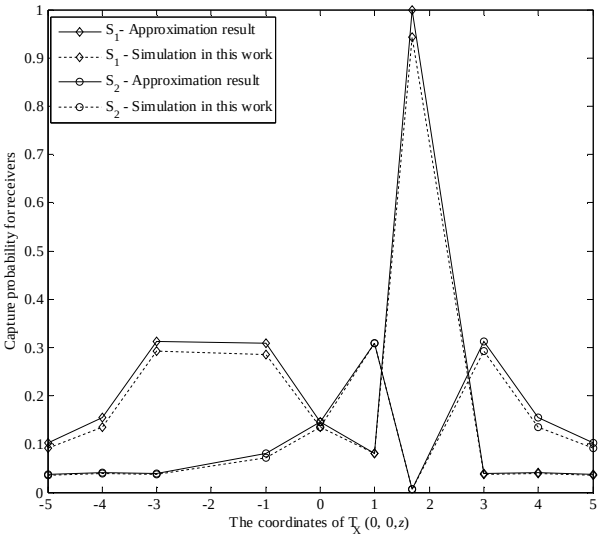

Fig. 2. Comparisons of capture probabilities between approximation and simulation results with a large simulation time.

the probability density function of $N_i = y$, $\mathrm{P_r}(N_i = y)$ can be derived as:

$$\begin{aligned}
\mathrm{P_r}\left(N_i = y\right) &= \sum_{x=0}^{N} \mathrm{P_r}\left(N_i = y \,|\, N_{0,i} = x\right) \mathrm{P_r}\left(N_{0,i} = x\right) \\
&= \sum_{x=0}^{N} \binom{N-x}{y} q^y (1-q)^{N-x-y} \binom{N}{x} p^x (1-p)^{N-x} \\
&= \left(q(1-p)\right)^y \sum_{x=0}^{N-y} \binom{N}{y} \binom{N-y}{x} p^x \left((1-p)(1-q)\right)^{N-y-x} \\
&= \binom{N}{y} \left(q(1-p)\right)^y \sum_{x=0}^{N-y} \binom{N-y}{x} p^x \left((1-p)(1-q)\right)^{N-y-x},
\end{aligned} \quad (8)$$

and then, by applying the Binomial theorem [20], we derive

$$\begin{aligned}
\mathrm{P_r}\left(N_i = y\right) &= \binom{N}{y} \left(q(1-p)\right)^y \left(p + (1-p)(1-q)\right) \\
&= \binom{N}{y} \left(q(1-p)\right)^y \left(1 - q(1-p)\right)^{N-y},
\end{aligned} \quad (9)$$

where $N_{0,i}$ is the number of molecules absorbed during $(0, i \cdot t_s)$, $N_{0,i} \sim \boldsymbol{N}(NP_i, NP_i(1 - P_i))$, $p = P_i = P_T(r_T, i \cdot t_s)$, and q is the probability that a molecule can be absorbed in the current time slot for the i^{th} transmission, i.e., $q = (P_{i+1} - P_i)/(1 - P_i)$, where $i = 1, 2, .. I$.

Equation (9) obviously shows that N_i follows a Binomial distribution:

$$N_i \sim \boldsymbol{B}\left(N, q(1-p)\right) \sim \boldsymbol{B}\left(N, P_{i+1} - P_i\right). \quad (10)$$

Due to the effects of ISI, the influence from previous consecutive symbols must be considered. However, the summation of Binomial distributions is hard to compute. Thus, N_0 and N_i can be approximated using the Gaussian approximation $N_{0;\mathrm{G}}$, $N_{i;\mathrm{G}}$ and the Poisson approximation $N_{0;\mathrm{P}}$, $N_{i;\mathrm{P}}$, respectively:

$$N_{0;\mathrm{G}} \sim \boldsymbol{N}\left(NP_1, NP_1(1-P_1)\right), \quad (11)$$

$$N_{0;\mathrm{P}} \sim \boldsymbol{P}\left(NP_1\right), \quad (12)$$

$$N_{i;\mathrm{G}} \sim \boldsymbol{N}\left(N\left(P_{i+1}-P_i\right), N\left(P_{i+1}-P_i\right)\left(1-P_{i+1}+P_i\right)\right) \sim \boldsymbol{N}\left(\varpi_i, \gamma_i\right), \tag{13}$$

$$N_{i;\mathrm{P}} \sim \boldsymbol{P}\left(N\left(P_{i+1}-P_i\right)\right), \tag{14}$$

where $\varpi_i = N(P_{i+1} - P_i)$ and $\gamma_i = N(P_{i+1} - P_i)(1 - P_{i+1} + P_i)$.

For a memory channel with an ISI length I, 2^I different bit sequences may be generated based on the different permutations of I previous information symbols. The total number of molecules received in the current time slot is composed of molecules sent at the start of the current time slot, and the number of molecules sent from the start of all I previous time slots. Thus, the total number of molecules received in the current time slot using the Gaussian and Poisson approximations, i.e., $N_{\mathrm{c;G}}$ and $N_{\mathrm{c;P}}$ respectively can be calculated as:

$$N_{\mathrm{c;G}} = a_{\mathrm{c}} N_{0;\mathrm{G}} + \sum_{i=1}^{I} a_{\mathrm{c}-i} N_{i;\mathrm{G}} \sim \boldsymbol{N}\left(a_{\mathrm{c}} N P_1 + \sum_{i=1}^{I} a_{\mathrm{c}-i}\varpi_i,\ a_{\mathrm{c}} N P_1\left(1-P_1\right) + \sum_{i=1}^{I} a_{\mathrm{c}-i}\gamma_i\right), \tag{15}$$

$$N_{\mathrm{c;P}} = a_{\mathrm{c}} N_{0;\mathrm{P}} + \sum_{i=1}^{I} a_{\mathrm{c}-i} N_{i;\mathrm{P}} \sim \boldsymbol{P}\left(a_{\mathrm{c}} N P_1 + \sum_{i=1}^{I} a_{\mathrm{c}-i} N\left(P_{i+1}-P_i\right)\right), \tag{16}$$

where $\{a_{\mathrm{c}-i},\ i = 0, 1, 2, .., I\}$ represents the transmitted information bits in binary form for the current and all previous I symbols.

An error occurs when there is a difference between the transmitted symbol and the received symbol. When '0' is transmitted, but '1' is received, the error probability for the Gaussian and Poisson approximations can be computed as:

$$P_{01;\mathrm{G},j} = {p_{\mathrm{tx}}}^{\alpha_j}\left(1-p_{\mathrm{tx}}\right)^{I+1-\alpha_j}\,\mathrm{P_r}\left(N_{\mathrm{c;G},j} > \tau\right) = {p_{\mathrm{tx}}}^{\alpha_j}\left(1-p_{\mathrm{tx}}\right)^{I+1-\alpha_j}\,\Phi\left(\frac{\mu_{01,j}-\tau}{\sigma_{01,j}}\right), \tag{17}$$

$$P_{01;\mathrm{P},j} = {p_{\mathrm{tx}}}^{\alpha_j}\left(1-p_{\mathrm{tx}}\right)^{I+1-\alpha_j}\,\mathrm{P_r}\left(N_{\mathrm{c;P},j} > \tau\right) = {p_{\mathrm{tx}}}^{\alpha_j}\left(1-p_{\mathrm{tx}}\right)^{I+1-\alpha_j}\left(1-\mathrm{Q}\left(\tau+1, \lambda_{01,j}\right)\right), \tag{18}$$

where:

$$\mu_{01,j} = \sum_{i=1}^{I} a_{\mathrm{c}-i,j}\varpi_i\ ,\ \sigma_{01,j} = \sqrt{\sum_{i=1}^{I} a_{\mathrm{c}-i,j}\gamma_i}\ ,\quad \lambda_{01,j} = \sum_{i=1}^{I} a_{\mathrm{c}-i,j} N\left(P_{i+1}-P_i\right), \tag{19}$$

$\{a_{\mathrm{c}-i,j}\ i = 1, 2, ..., I\}$ is the binary message sequence of the bit sequence j, and $j = 1, 2, \ldots, 2^I$, is the bit sequence index. p_{tx} is the transmitted probability of bit '1'. $\mathrm{P_r}(N_{\mathrm{c;G/P},j} > \tau)$ is the probability of $N_{\mathrm{c;G/P},j} > \tau$, and α_j is the number of '1's in the bit sequence j. $\Phi(\cdot)$ is the cumulative distribution function of standard Gaussian distribution, and $\mathrm{Q}(\cdot)$ is the regularized gamma function.

Conversely, when a '1' is transmitted, but a '0' is received, the error probability for the Gaussian and Poisson approximations can be given as:

$$P_{10;\mathrm{G},j} = {p_{\mathrm{tx}}}^{\alpha_j+1}\left(1-p_{\mathrm{tx}}\right)^{I-\alpha_j}\,\mathrm{P_r}\left(N_{\mathrm{c;G},j} \le \tau\right) = {p_{\mathrm{tx}}}^{\alpha_j+1}\left(1-p_{\mathrm{tx}}\right)^{I-\alpha_j}\,\Phi\left(\frac{\tau-\mu_{10,j}}{\sigma_{10,j}}\right). \tag{20}$$

$$P_{10;\mathrm{P},j} = {p_{\mathrm{tx}}}^{\alpha_j+1}\left(1-p_{\mathrm{tx}}\right)^{I-\alpha_j}\,\mathrm{P_r}\left(N_{\mathrm{c;P},j} \le \tau\right) = {p_{\mathrm{tx}}}^{\alpha_j+1}\left(1-p_{\mathrm{tx}}\right)^{I-\alpha_j}\,\mathrm{Q}\left(\tau+1, \lambda_{10,j}\right). \tag{21}$$

where:

$$\mu_{10,j} = NP_1 + \sum_{i=1}^{I} a_{\mathrm{c}-i,j}\varpi_i,\ \ \sigma_{10,j} = \sqrt{NP_1\left(1-P_1\right) + \sum_{i=1}^{I} a_{\mathrm{c}-i,j}\gamma_i}\,. \quad \lambda_{10,j} = NP_1 + \sum_{i=1}^{I} a_{\mathrm{c}-i,j} N\left(P_{i+1}-P_i\right). \tag{22}$$

Thus, the BER for the target link, P_{Te}, can be derived as:

$$P_{\mathrm{Te}} = P_{01} + P_{10} = \sum_{j=1}^{2^I}\left(P_{01;\mathrm{G/P},j} + P_{10;\mathrm{G/P},j}\right), \tag{23}$$

where $P_{01;\mathrm{G/P},j} = P_{01;\mathrm{G},j}$ or $P_{01;\mathrm{P},j}$ and $P_{10;\mathrm{G/P},j} = P_{10;\mathrm{G},j}$ or $P_{10;\mathrm{P},j}$. The selection is based on the approximation model that will be used for the analysis in the designed system.

Consider that the binary input and the output of the single channel can be represented as $\mathrm{X} = \{X_1, X_2, \ldots, X_k\}$ and $\mathrm{Y} = \{Y_1, Y_2, \ldots, Y_k\}$ respectively. Therefore, the capacity of the memory channel for a system with an impulsive on-off keying scheme can be calculated as [21, Eq. (1.2)]:

$$C = \lim_{k\to\infty} \max_{p_{\mathrm{tx}}} \sum_{i=1}^{k} \frac{1}{k} \mathbf{I}\left(X_i; Y_i\right), \tag{24}$$

where $\mathbf{I}(X_i;Y_i)$ is the mutual information defined as [22, Eq. (5)]:

$$\mathbf{I}\left(X_i;Y_i\right) = H\left(Y_i\right) - H\left(Y_i \mid X_i\right) = \mathbf{H}\left(\left(1-p_{\mathrm{tx}}\right)\left(1-P_{01}\right) + p_{\mathrm{tx}}P_{10}\right) - p_{\mathrm{tx}}\mathbf{H}\left(1-P_{10}\right) - \left(1-p_{\mathrm{tx}}\right)\mathbf{H}\left(1-P_{01}\right), \tag{25}$$

where $\mathbf{H}(\delta) = -\delta\log_2\delta - (1-\delta)\log_2(1-\delta)$.

For a memory channel with an ISI length I, after the I^{th} symbol, the detection of emitted molecular signal will be affected by the I most recent previous signals. According to (17)-(23), it can be deduced that the average error probability stays constant after the I^{th} symbol, thus:

$$\mathbf{I}\left(X_i;Y_i\right) = \mathbf{I}\left(X_{I+1};Y_{I+1}\right),\ I < i \le k\ . \tag{26}$$

Therefore, for the memory limited channel, the channel capacity can be simplified as:

$$
\begin{aligned}
C &= \lim_{k\to\infty} \max_{p_{tx}} \sum_{i=1}^{k} \frac{1}{k} \mathbf{I}\left(X_i;Y_i\right) \\
&= \lim_{k\to\infty} \max_{p_{tx}} \left(\sum_{i=1}^{I} \frac{1}{k} \mathbf{I}\left(X_i;Y_i\right) + \sum_{i=I+1}^{k} \frac{1}{k} \mathbf{I}\left(X_i;Y_i\right) \right) \\
&= 0 + \lim_{k\to\infty} \max_{p_{tx}} \left(\frac{k-I}{k} \mathbf{I}\left(X_{I+1};Y_{I+1}\right) \right) \\
&= \max_{p_{tx}} \left(\mathbf{I}\left(X_{I+1};Y_{I+1}\right) \right).
\end{aligned} \tag{27}
$$

The channel capacity for the target link with the Gaussian and Poisson approximations can be derived by substituting the corresponding equations for each approximation into (27).

IV. Numerical Results for the First Study

In this section, the numerical results for the first study are presented. The capture probability of R_T, and the BER and capacity of the target link are given based on the simulation and theoretical derivation. The performance of a PTP communication system is compared against a single receiver, R_S, where the transmission distance between T_X and R_S is r_S = 7μm. The set of simulation parameters is shown in Table I.

The T_X and R_T are placed in fixed positions (0, 0, 0) and (0, 0, 7μm), and the coordinates of R_I (0, 0, z_I,) are variable with $z_I \in \{-7, -4, -2, 2, 4, 10, 12, 14\}$ μm. We denote r_I-, r_I+ and r_I++ as the distance between the T_X and R_I in Scenarios 1, 2, and 3, respectively.

Using the simulation process introduced in Section II, the capture probabilities of R_T with different positions of R_I and R_S are illustrated in Fig. 3. The results show that all capture probabilities increase with increasing simulation time. When the simulation time is long enough, the capture probability appears to converge. It can also be seen that for different positions of R_I, the capture probabilities of R_T are different. They are all smaller than the capture probability of R_S. For the two-receiver system, the maximum and minimum values of capture probabilities of R_T occur in Scenario 3 with r_I++ = 14μm, and Scenario 2 with r_I+ = 2μm respectively. These results illustrate that the capture ability of R_T is weakened and have thus shown the different levels of impact due to the existence of R_I. This is because R_I absorbs information molecules that could have arrived at R_T. Furthermore, for different positions of R_I, the ability to absorb the information molecules is different which is also reflected in the values of capture probabilities of R_T. Finally, the R_I has the greatest impact when it is literally blocking the R_T, i.e., when R_I is placed between T_X and R_T. These results demonstrate that treating the two-receiver molecular communication as two PTP molecular communication models is inappropriate.

In Section III, the BER and channel capacity were analyzed for the Gaussian and Poisson approximations. In order to determine which approximation is more accurate for this work, the cumulative density functions (CDFs) of the number of received molecules for the Gaussian and Poisson models are compared with the CDF of the simulation results. The Root Mean Squared Error (RMSE) is introduced as follows [24, Eq. (8)]:

TABLE I
Parameters setting

Parameters	Definition	Value
D	Diffusion coefficient	79.4μm²/s
r_{ra}	Radius of receivers	1μm
Δt	Time step	0.0001s
$r_{I,}$	Distance between T_X and R_I	Variable
r_T	Distance between T_X and R_T	7μm
r_S	Distance between Tx and R_S	7μm
I	ISI length	10 [23]
$(x_0, y_{0,} z_0)$	Coordinate of T_X	(0, 0, 0)
$(0, 0, z_I)$	Coordinate of R_I	Variable
$(0, 0, z_T)$	Coordinate of R_T	(0, 0, 7μm)

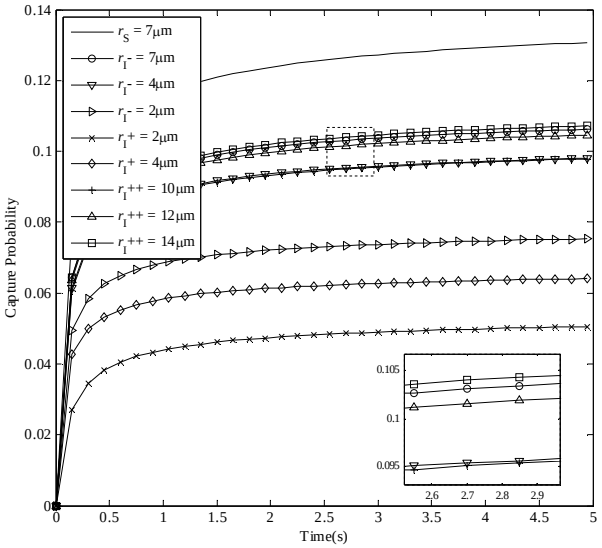

Fig. 3. The comparisons of capture probabilities between R_T and R_S.

$$
\mathrm{RMSE} = \sqrt{\frac{1}{N+1} \sum_{x_i=0}^{N} \left(\mathrm{CDF}_{\mathrm{sim}}\left(x_i\right) - \mathrm{CDF}_{\mathrm{G/P}}\left(x_i\right) \right)^2}, \tag{28}
$$

where $\mathrm{CDF}_{\mathrm{sim}}$ and $\mathrm{CDF}_{\mathrm{G/P}}$ are CDFs of the simulation results and the Gaussian or Poisson model results, respectively.

Figs. 4 (a) and 4 (b) show the RMSE of CDFs for PTP system with r_S= 7μm and the two-receiver system with r_T = 7μm, respectively. The results indicate that the RMSE of the Poisson model is more stable as N varies. However, the Gaussian model obviously improves with increasing N. As shown in Fig. 4(a), the Poisson model is more accurate for N < 4000, after which the Gaussian model is better. The BER against the number of molecules per bit is also presented in this figure. When N < 4000, a BER level as low as 10^{-9} can be measured for both the Gaussian and Poisson models. In this case, the Poisson model is preferred for a PTP communication system based on the lower RMSE values. For the target link of the two-receiver system in Fig. 4(b), the RMSEs are measured for different distances of R_I. The results show that the values of the RMSE of the Poisson model are always lower than the values obtained from the Gaussian model for N = 0 ~ 10000. Thus, the Poisson approximation is considered in this analysis.

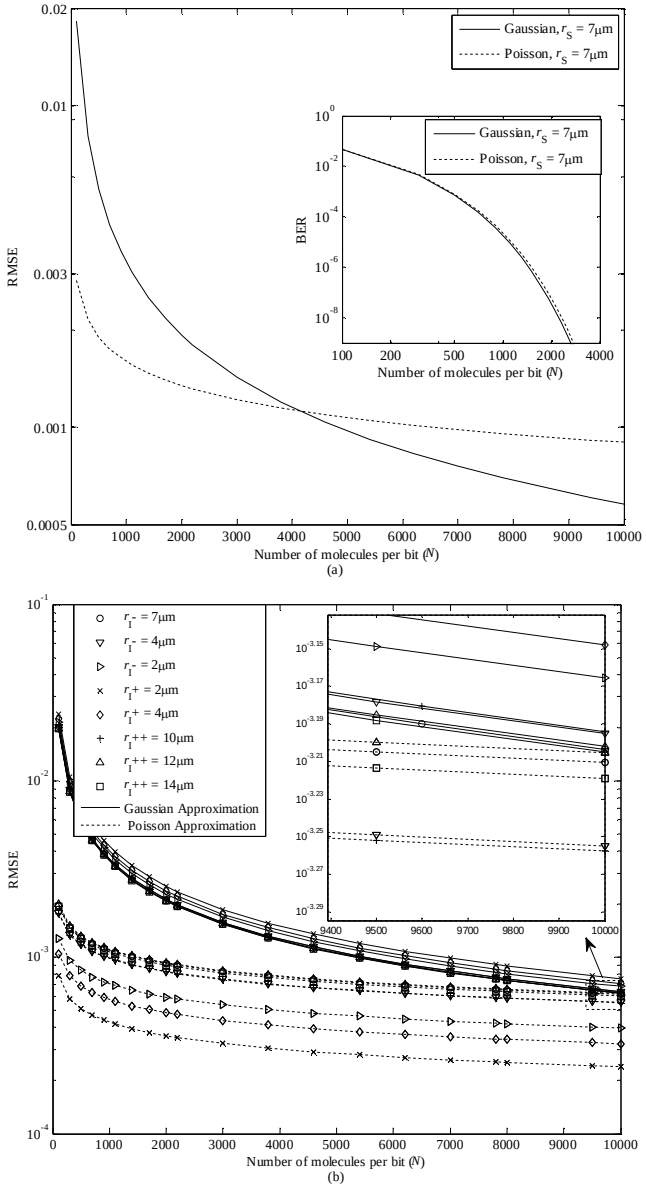

Fig. 4. RMSE of CDFs for (a) PTP system with r_S = 7μm (b) Two-receiver system with r_T = 7μm.

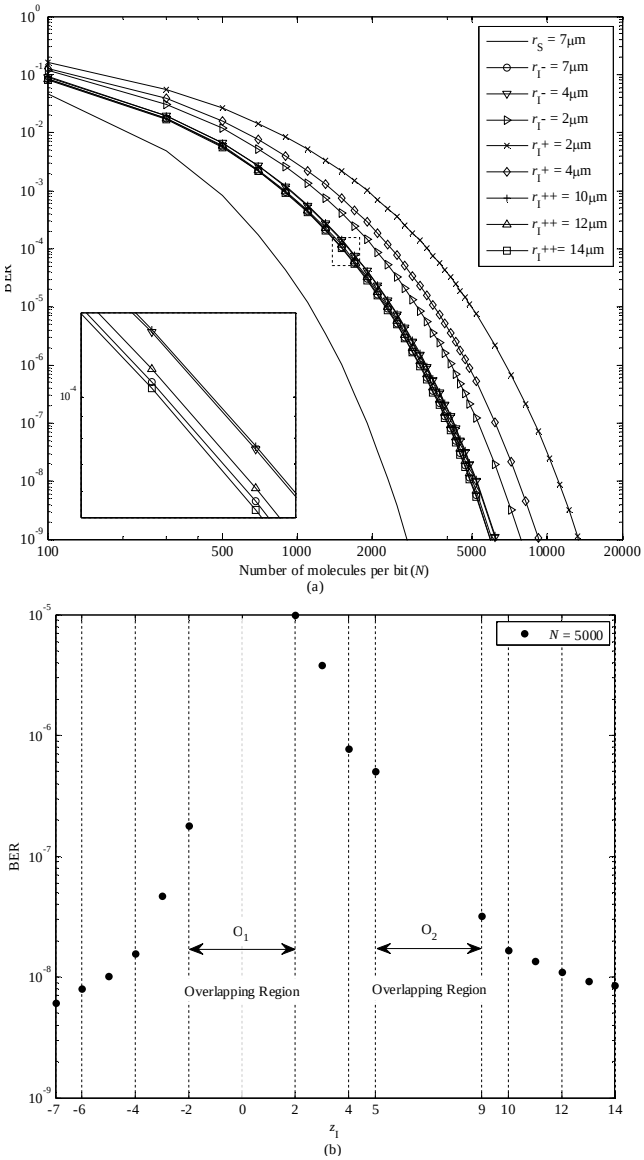

Fig. 5. (a) BER comparisons between the target link with different positions of R_I and the PTP system, p_{tx} = 0.5 (b) BER with different values of z_I at N = 5000.

The BERs and capacities of the target link of the two-receiver system with r_T = 7μm and the PTP system with r_S = 7μm are presented in Fig. 5(a) and Fig. 6. The numerical results clearly show that increasing the number of molecules leads to a lower BER and higher capacity. The performance ranking is consistent with the capture probabilities show in Fig. 3. Thus, the lowest BER and also the highest capacity is provided by the PTP system, and the lowest and highest BERs of the target link occur in Scenario 3 with r_I++ = 14μm and Scenario 2 with r_I+ = 2μm, respectively. The BERs at N = 5000 for different values of z_I are shown in Fig. 5(b). O_1 and O_2 are the regions that R_I overlaps with the T_X and R_T respectively. The overlap between R_I and T_X or R_I and R_T is physically unrealizable, thus, these two regions are not considered. This figure directly shows the BER trend of the target link with varying positions of R_I. As R_I changes position from Scenario 1 to Scenario 2 to Scenario 3, the BER increases at first and when it arrives at the closest position to T_X in Scenario 2, the BER reaches a maximum, and then the BER decreases. Both BER and capacity imply that the R_I's existence does reduce the reliability of the target link, and due to the significant impact, the positions of the R_I in Scenario 2 are especially undesirable for R_T, where the reliability of the target link is the worst of the three Scenarios. In Scenario 2, the R_T is effectively blocked by R_I, and the capture ability of R_I and R_T reach their highest level and lowest level, respectively. Thus, the worst performance of R_T is obtained. The impact of R_I in Scenario 1 and Scenario 3 are very similar, except when r_I- = 2μm, i.e., when the R_I is very close to the T_X. The distance variations of R_I in Scenario 3 and Scenario 2 cause the smallest and the biggest change in both BER and capacity respectively. The increase in distance between R_I and T_X leads to decreasing and increasing the capture probability of R_I and R_T respectively. Thus, in each scenario, the further the distance between the R_I and T_X, the less the impact on R_T.

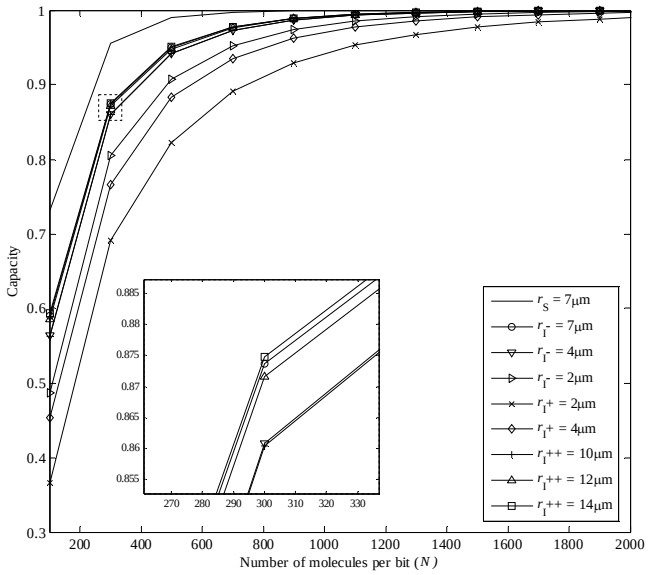

Fig. 6. Channel capacity comparisons between the target link with different positions of R_I and the PTP system.

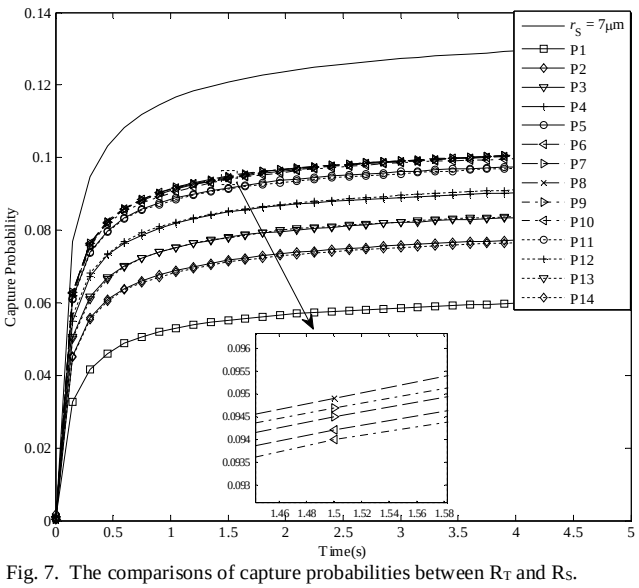

Fig. 7. The comparisons of capture probabilities between R_T and R_S.

V. Numerical Results for the Second Study

In this section, the second study of the effect of positions of R_I on R_T is presented. Similar to the first study, the numerical results focus on the capture probability of the R_T, and the BER and channel capacity of the target link. A comparison of these results between the two-receiver system and the PTP system are also presented. In the simulation, r_I = 5μm, and the coordinate of R_I, (x_I, 0, z_I) is variable. All other parameters are the same as in Table I.

As shown in Fig. 1(b), the T_X and R_T are placed in fixed positions (0, 0, 0) and (0, 0, 7μm), and R_I is placed on a circle that is located in the *xz*-plane and centered at the origin. To distinguish these scenarios from those that were considered in the first study, here, the four scenarios are labeled as Scenario 4 to Scenario 7. The scenarios and the corresponding positions of R_I are shown in Table II.

In this study, the position of R_I is changing from P1 to P14 in sequence. Fig. 7 shows the comparisons of capture probabilities between R_T with different positions of R_I and R_S. As in the previous study, a PTP molecular communication system gives the maximum value of capture probability. The best and worst case in the two-receiver system occurs in P8 and P1 respectively. When varying the positions of R_I according to above order, the distance between R_I and R_T increases first and when R_I is placed in P8, the distance between R_I and R_T reach the maximum value, after that, this distance begins to decreases. The increase of the distance between R_I and R_T leads to an increasing of the capture probability of R_T. On the contrary, the decrease of this distance increases the impact of R_I on R_T which results in a decreasing of the capture probability of R_T. In addition, the values of capture probability of R_T are very similar when R_I arrives at those positions which are symmetrical about the *z*-axis (e.g. P2 and P14). The positions of R_I in Scenario 5 and Scenario 6 change to the capture probabilities of R_T are fairly minor compare with positions in Scenario 4 and 7. This is because the positions of R_I in Scenario 4 and Scenario 7 will be easier for the R_I to capture the information molecules that could be absorbed by R_T, especially when R_I is located at P1.

TABLE II
Scenarios and positions

Scenario 4	Scenario 5	Scenario 6	Scenario 7
P1(0,0,5)	P6(4,0,-3)	P9(-3,0,-4)	P11(-5,0,0)
P2(2,0,4.58)	P7(3,0,-4)	P10(-4,0,-3)	P12(-3,0,4)
P3(3,0,4)	P8(0,0,-5)		P13(-3,0,4)
P4(4,0,3)			P14(-2,0,4.58)
P5(5,0,0)			
Unit: μm			

On the basis of the above analysis, the capture probability curves from P6 to P10 are very similar and differ only slightly from each other. Thus the changes of positions of R_I in Scenario 5 and 6 have similar effects on R_T. In addition, the capture probabilities of R_T are very similar when positions of R_I are symmetrical about the *z*-axis. Therefore, for the remainder of this work, only P1, P2, P3, P4, P5 and P8 are needed for the analysis of BER and channel capacity of the target link.

The RMSE as a decision metric was used in Section IV to determine which approximation is suitable for the proposed system. Employing the same decision method, the Poisson approximation is also selected for use in this study. Fig. 8(a) and Fig. 9 show the BER and capacity of the target link when considering different positions of R_I. The results indicate that an increase in the distance between R_I and R_T leads to decreasing BER and increasing capacity. The worst and the best performance occurs in P1 and P8, respectively. Fig. 8(b) show the BER of the target link with different positions of R_I at N = 5000, it clearly shows a BER trend of the target link with the varying positions of R_I. As the position of R_I changes from scenario 4 to Scenario 5 to Scenario 6 to Scenario 7, the BER decreases first and when it arrives at the farthest distance from R_T, which is P8, the lowest BER is obtained and after that, with

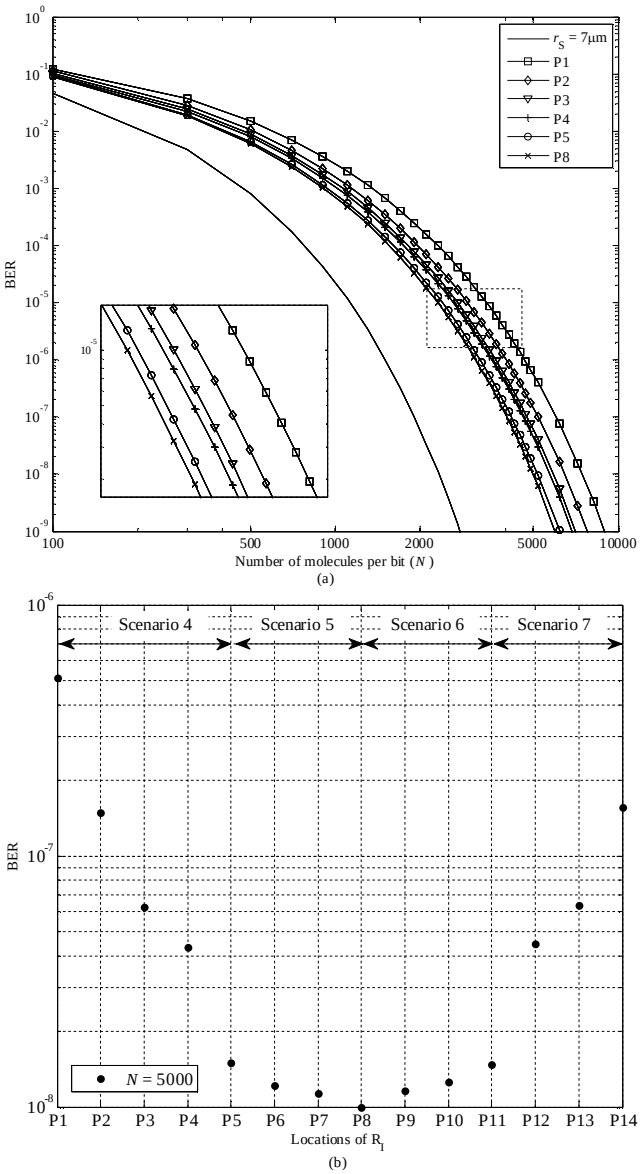

Fig. 8.(a) BER comparisons between the target link with different positions of R_I and the PTP system, p_{tx} = 0.5 (b) BER with different positions of R_I at N = 5000.

decreasing distance between R_I and R_T, the BER increases again. This study illustrates that when considering the positions of R_I that have the same distance from T_X, the further the distance between R_I and R_T, the less the impact on R_T.

VI. Conclusion

In this paper, the two-receiver broadcast channel for molecular communications system has been simulated and the idea of an interferer node R_I and the effect of its location on R_T are introduced. The channel model was then analyzed with both the Gaussian approximation and the Poisson approximation. The RMSE [24] is applied as a metric to determine which approximation is better for the system. Here, two studies of the effect of positions of R_I on R_T are provided. Through the simulation and theoretical derivations, the impact of the

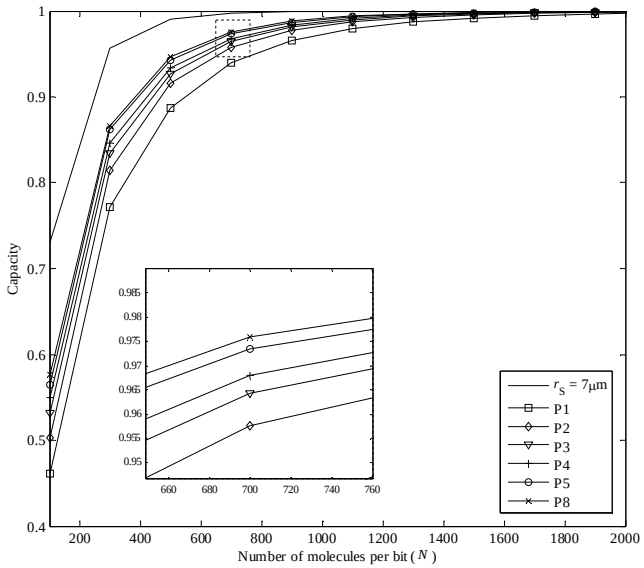

Fig. 9. Channel capacity comparisons between the target link with different positions of R_I and the PTP system.

position of R_I on R_T is shown via the BER and channel capacity of the target link. The results indicate that different positions of R_I relative to T_X and R_T have varying effects on R_T, especially when the R_T is completely blocked by R_I, i.e., the positions in Scenario 2 and P1 in Scenario 4. In addition, for all scenarios, the further the R_I is away from T_X or R_X, the better performance of the target link can be achieved. Furthermore, the performance of the target link of the two-receiver system is always worse than the performance of the PTP system when considering the same parameters. Therefore, the use of the PTP approximation should not be used for a broadcast system with absorbing receivers as it cannot guarantee, or predict, the reliability of the signal at a given receiver.

It can also be concluded from this work that these new findings should open up further avenues of research. The absorbing receiver is in fact an idealization in comparison to binding receivers (either reversibly or irreversibly) with finite kinetic rates and thus the results here provide an upper bound on the performance degradation due to the interfering receiver. Thus, there would be some interesting work to carry out in understanding the design and placement more specifically for an absorbing receiver as found in drug delivery systems as the design may limit the side effects of the drug delivery system [25].

Furthermore, whilst the focus of this paper has been at the physical layer, further work is also possible at other levels of the stack. Particular interest may be found in optimizing the addressing scheme to minimize the effects from the interfering receivers [26]. In addition, emphasis on either the hidden and/or exposed receiver, as typical concepts of wireless networks, can also be investigated.

Finally, this work, has introduced to the literature the notion of a single interfering receiver but naturally, extensions can be seen found in analyzing multiple interfering receivers at all layers of the stack.

REFERENCES

[1] I. F. Akyildiz, F. Brunetti, and C. Blázquez, "Nanonetworks: A new communication paradigm," *Comput. Netw.*, vol. 52, pp. 2260-2279, Aug. 2008.

[2] M. Pierobon and I. F. Akyildiz, "A physical end-to-end model for molecular communication in nanonetworks," *IEEE J. Sel. Areas Commun.*, vol. 28, pp. 602-611, May 2010.

[3] M. Ş. Kuran, H. B. Yilmaz, T. Tugcu, and B. Özerman, "Energy model for communication via diffusion in nanonetworks," *Nano Commun. Netw.*, vol. 1, pp. 86-95, Jun. 2010.

[4] M. Ş. Kuran, H. B. Yilmaz, T. Tugcu, and I. F. Akyildiz, "Modulation Techniques for Communication via Diffusion in Nanonetworks," in *IEEE Int. Conf. Commun. (ICC)*, Jun. 2011, pp. 1-5.

[5] M. Pierobon and I. F. Akyildiz, "Capacity of a Diffusion-Based Molecular Communication System With Channel Memory and Molecular Noise," *IEEE Trans.Inf. Theory.*, vol. 59, pp. 942-954, Feb 2013.

[6] H. ShahMohammadian, G. G. Messier, and S. Magierowski, "Optimum receiver for molecule shift keying modulation in diffusion-based molecular communication channels," *Nano Commun. Netw.*, vol. 3, pp. 183-195, Sep. 2012.

[7] H. B. Yilmaz, A. C. Heren, T. Tugcu, and C. B. Chae, "Three-Dimensional Channel Characteristics for Molecular Communications With an Absorbing Receiver," *IEEE Commun. Lett.*, vol. 18, pp. 929-932, Jun. 2014.

[8] C. Lee, B. Koo, N. R. Kim, B. Yilmaz, N. Farsad, A. Eckford, *et al.*, "Molecular MIMO communication link," in *IEEE Comput. Communi. Workshops (INFOCOM WKSHPS)*, May. 2015, pp. 13-14.

[9] L. S. Meng, P. C. Yeh, K. C. Chen, and I. F. Akyildiz, "MIMO communications based on molecular diffusion," in *IEEE Global Commun. Conf. (GLOBECOM)*, Dec. 2012, pp. 5380-5385.

[10] B. H. Koo, C. Lee, H. B. Yilmaz, N. Farsad, A. Eckford, and C. B. Chae, "Molecular MIMO: From Theory to Prototype," *IEEE J. Sel. Areas Commun.*, vol. 34, pp. 600-614, Mar. 2016.

[11] B. Atakan and O. B. Akan, "On molecular multiple-access, broadcast, and relay channels in nanonetworks," in *Proc. ICST BIONETICS*, Japan, Dec. 2008, pp. 1-8.

[12] S. F. Bush, *Nanoscale Communication Networks*: Artech House, 2010.

[13] W. Guo, C. Mias, N. Farsad and J. L. Wu "Molecular Versus Electromagnetic Wave Propagation Loss in Macro-Scale Environments," *IEEE Trans. Mol. Biol. Multi-Scale Commun.*, vol 1, pp. 18-25, Nov. 2015.

[14] H. C. Berg, *Random Walks in Biology*: Princeton University Press, 1993.

[15] L. Felicetti, M. Femminella, G. Reali, T. Nakano, and A. V. Vasilakos, "TCP-like molecular communications," *IEEE J. Sel. Areas Commun.*, vol. 32, pp. 2354-2367, 2014.

[16] H. ShahMohammadian, G. G. Messier, and S. Magierowski, "Blind synchronization in diffusion-based molecular communication channels," *IEEE commun. Lett.*, vol. 17, pp. 2156-2159, 2013.

[17] M. S. Leeson and M. D. Higgins, "Error correction coding for molecular communications," in *IEEE Int. Conf. Commun.(ICC)*, 2012, pp. 6172-6176.

[18] H. Sano, "Solutions to the Smoluchowski equation for problems involving the anisotropic diffusion or absorption of a particle," *The J. Chem. Phys.*, vol. 74, pp. 1394-1400, Jan. 1981.

[19] W. Mendenhall, R. Beaver, and B. Beaver, *Introduction to Probability and Statistics*: Cengage Learning, 2012.

[20] F. P. Miller, A. F. Vandome, and M. B. John, *Binomial Theorem: Exponentiation, Summation, Natural Number, Pascal's Triangle, Formula, Combinatorics, Element (mathematics), Set (mathematics), Binomial Coefficient, Binomial Distribution*: VDM Publishing, 2010.

[21] S. Verdú and H. Te, "A general formula for channel capacity," *IEEE Trans. Inf. Theory*, vol. 40, pp. 1147-1157, Jul. 1994.

[22] T. Nakano, Y. Okaie, and L. Jian-Qin, "Channel Model and Capacity Analysis of Molecular Communication with Brownian Motion," *IEEE Commun. Lett.*, vol. 16, pp. 797-800, Jun. 2012.

[23] Y. Lu, M. D. Higgins, and M. S. Leeson, "Comparison of Channel Coding Schemes for Molecular Communications Systems," *IEEE Trans. Commun.*, vol 63, pp. 3991-4001, Nov. 2015.

[24] H. B. Yilmaz and C. Chan-byoung, "Arrival modelling for molecular communication via diffusion," *Electron. Lett.*, vol. 50, pp. 1667-1669, Nov. 2014.

[25] L. Felicetti, M. Femminella, G. Reali, and P. Liò, "Applications of molecular communications to medicine: A survey," *Nano Commun. Netw.*, vol. 7, pp. 27-45, March 2016.

[26] T. Nakano, T. Suda, Y. Okaie, M. J. Moore, and A. V. Vasilakos, "Molecular communication among biological nanomachines: A layered architecture and research issues," *IEEE Trans. Nanobiosci.*, vol. 13, pp. 169-197, Sept. 2014.

Yi Lu received the degree of Bachelor of Engineering with First Class Honors in Electronic Engineering from University of Central Lancashire, UK, in 2011. And then she obtained a Master degree of Engineering with Distinction in Electronic Engineering from University of Sheffield, UK, in 2012. She is currently a scholarship student pursuing a PhD study in Nano-communications at University of Warwick.

Matthew D. Higgins received his MEng in Electronic and Communications Engineering and his PhD in Engineering from the School of Engineering at the University of Warwick in 2005 and 2009 respectively. Remaining at the University of Warwick, he then progressed through several Research Fellow positions, in association with some of the UKs leading defence and telecommunications companies before undertaking two years as a Senior Teaching Fellow in Telecommunications, Electrical Engineering and Computer Science subjects. In July 2012, Dr Higgins was promoted to the position of Assistant Professor where his research focused on Optical, Nano, and Molecular Communications. As of March 2016, Dr Higgins was appointed as an Associate Professor at WMG working in the area of Connected and Autonomous Vehicles.

Adam Noel received the B.Eng. degree in Electrical Engineering in 2009 from Memorial University in St. John's, Canada, the M.A.Sc. degree in Electrical Engineering in 2011 from the University of British Columbia (UBC) in Vancouver, Canada, and the Ph.D. degree in Electrical and Computer Engineering in 2015 from UBC. In 2013 he was a Visiting Scientist at the Institute for Digital Communication at Friedrich-Alexander-University in Erlangen, Germany. He is currently a Postdoctoral Fellow at the University of Ottawa, Canada. Dr. Noel's current research interests include channel modelling, system design, and simulation methods for molecular communication networks. He is a Member of the IEEE.

Mark S. Leeson received the degrees of BSc and BEng with First Class Honors in Electrical and ElectronicEngineering from the University of Nottingham, UK, in 1986. He then obtained a PhD in Engineering from the University of Cambridge, UK, in 1990. From 1990 to 1992 he worked as a Network Analyst for National Westminster Bank in London. After holding academic posts in London and Manchester, in 2000 he joined the School of Engineering at Warwick, where he is now a Reader. His major research interests are coding and modulation, molecular communications, optical communication systems and evolutionary optimisation. To date, Dr Leeson has over 230 publications and has supervised fifteen successful research students. He is a Senior Member of the IEEE, and a Fellow of both the UK Institute of Physics and the UK Higher Education Academy.

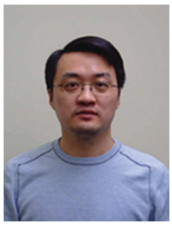

Yunfei Chen received his B.E. and M.E. degrees in electronics engineering from Shanghai Jiaotong University, Shanghai, P.R.China, in 1998 and 2001, respectively. He received his PhD. degree from the University of Alberta in 2006. He is currently working as an Associate Professor at the University of Warwick, U.K. His research interests include wireless communications, cognitive radios, wireless relaying and energy harvesting.